Electronics and Communications in Japan, Part 3, Vol. 83, No. 1, 2000
Translated from Denshi Joho Tsushin Gakkai Ronbunshi, Vol. J80-A, No. 10, October 1997, pp. 1654–1659

Micromanipulation Using a Focused Ultrasonic Standing Wave Field

Teruyuki Kozuka, Toru Tuziuti, and Hideto Mitome

National Industrial Research Institute of Nagoya, Agency of Industrial Science and Technology, Ministry of International Trade and Industry, Nagoya, Japan 462-8510

Toshio Fukuda

Nagoya University, Nagoya, Japan 464-8603

SUMMARY

The authors present an experimental study of noncontact manipulation of small particles using the force caused by acoustic radiation pressure. An ultrasonic standing wave field was generated in water between a concave spherical transducer and a plane reflector placed at the focal point and suspended alumina particles were trapped on the central axis of the transducer. Moreover, the trapped particles were transported one-dimensionally along the sound beam axis by changing the frequency. By selecting the frequency increment, the agglomerated particle column was separated at different positions. The trapped particles can be transported through a distance of a few millimeters with submicrometer resolution. © 1999 Scripta Technica, Electron Comm Jpn Pt 3, 83(1): 53–60, 2000

Key words: Acoustic radiation pressure; focused ultrasound; standing wave; small particle; manipulation.

1. Introduction

In the research and development of micromachines, technology of noncontact manipulation of small particles is making progress [1, 2]. In filtering of powders of raw materials which is the basic process of new material development, noncontact handling technology to select the powder according to its characteristics is also needed. Electrostatic force [3] and radiation pressure of laser light [4] are widely used to apply the force without contact but acoustic radiation pressure of ultrasound may also be used and there are various reports about its application [5–8].

When an ultrasonic wave propagating in a fluid is obstructed by an object a pushing force in the direction of sound propagation appears on the object [9]. This force originates from acoustic radiation pressure which can be used to apply the force on the object without contact. If one injects small suspended particles into a standing wave field generated between a transducer and a reflector, then trapping and agglomeration occur at the nodes of sound pressure distribution. If the sound field is changed under this condition, the position of trapped particles changes. But in the experiment using a plane-type transducer, control of trapping position of small particles was difficult, since the range of action was distributed in front of the transducer in a wide range [10].

Using a concave spherical transducer, the sound field can be focused up to the order of wavelength. If one uses a standing wave field generated between the concave spherical transducer and a reflector placed at its focal point, objects which are sufficiently small compared to the wavelength can be manipulated along the sound beam axis. In research on particle manipulation using a focused ultrasound, Wu and Du [11, 12] have trapped small particles and frog eggs of the order of the wavelength in the potential well generated at the focal point of a focused traveling wave field. Here, by changing the frequency, the position of the focal point was changed and the trapped particles were moved. To suppress the effect of acoustic streaming, its experimental setup consisted of two focused transducers facing each other, which is quite similar to the experimental apparatus of this paper but the principles and size of the objects treated here are different. In this paper, using the standing wave field of the focused ultrasound generated between the concave spherical transducer and the reflector, the alumina particles suspended in water are trapped one-dimensionally at the nodes of the sound pressure distribution generated at intervals of a half-wavelength along the sound beam axis. By changing the frequency, the interval between the sound pressure nodes is changed and position control of the trapped object is realized. Moreover, the effects of the curvature of the concave transducer and the frequency are investigated.

2. Sound Field

According to Nyborg [13] and Gor'kov [14], the force acting on a small sphere due to radiation pressure can be given by the following equation, provided the radius a of the sphere is sufficiently small compared to the wavelength λ ($ka << 1$, $k = 2\pi/\lambda$):

$$F = V\left[B\nabla < K_a > -(1-\gamma)\nabla < P_a >\right] \tag{1}$$

Where V [$= (4/3)\ \pi a^3$] is the volume of the small sphere, $<K_a>$ and $<P_a>$ are the time averaged kinetic energy and potential energy of sound acting on the small sphere, respectively, and ∇ is the gradient operator. B [$= 3(\rho - \rho_0) / (2\rho + \rho_0)$] is given by the density ρ_0 and ρ of the medium and the small sphere, and γ ($= \beta/\beta_0$) is the ratio of compressibility of the medium β_0 and that of the small sphere β, respectively.

To study the force experienced by an object in the sound field, the potential U of the radiation force per unit volume is introduced by the following equations:

$$F/V = -\nabla U \tag{2}$$

$$U = -B < K_a > +(1-\gamma) < P_a > \tag{3}$$

Here the small sphere placed in the sound field experiences a force directed toward the potential well.

Consider the standing wave field generated in the medium of sound speed c_0 by the interference of sinusoidal plane sound waves having a sound pressure amplitude of A and frequency f. The sound beam axis is taken along the x-axis. If the potential of the particle velocity along the y-axis, which is perpendicular to the sound beam axis, has the distribution $g(y)$, $<K_a>$ and $<P_a>$ can be expressed as

$$< K_a >= g(y)^2 \frac{A^2}{\rho_0 {c_0}^2} \cos^2 kx \tag{4}$$

$$< P_a >= g(y)^2 \frac{A^2}{\rho_0 {c_0}^2} \sin^2 kx \tag{5}$$

where $k = 2\pi f/c_0$. Then, Eq. (3) becomes

$$U = g(y)^2 \frac{A^2}{\rho_0 {c_0}^2}\left\{-B + (B + 1 - \gamma)\ \sin^2 kx\right\} \tag{6}$$

If $g(y)$ has the Gaussian distribution given by

$$g(y) = \exp(-y^2/2\sigma^2) \tag{7}$$

the potential with variance $\sigma^2 = 1$ is distributed as in Fig. 1 where the medium is water ($\rho_0 = 1.0 \times 10^3$ kg/m^3, $c_0 = 1.5 \times 10^3$ m/s, $\beta_0 = 4.44 \times 10^{-10}$ s^2 m/kg) and the particles are alumina ($\rho = 3.95 \times 10^3$ kg/m^3, $c = 1.05 \times 10^4$ m/s, $\beta = 2.28 \times 10^{-10}$ s^2 m/kg). This potential varies with a period of a half-wavelength along the sound beam axis x. The potential takes maximum values at the antinodes of the sound pressure in the direction perpendicular to the sound axis, while it takes minimum values at the nodes. Thus, a small object placed in the sound field experiences a repulsive force from the antinodes of the sound pressure and an attractive force from the nodes, and stable points occur at half-wavelength intervals along the sound beam axis.

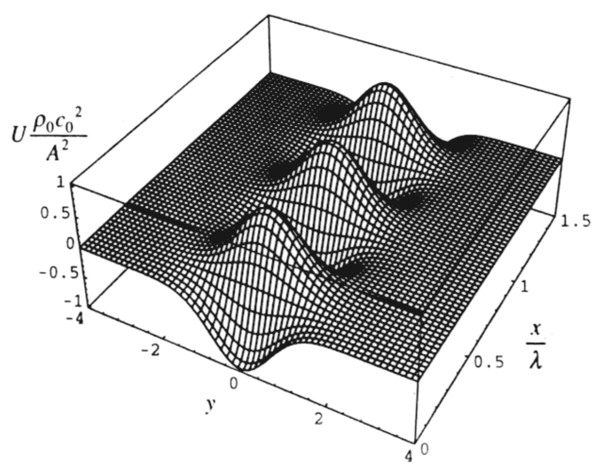

Fig. 1. Distribution of potential of acoustic radiation force in a standing wave field.

Takeuchi [15] showed that a small sphere is trapped at the nodes of the sound pressure distribution of the standing wave field when $B + 1 - \gamma > 0$, while it is trapped at the antinodes when $B + 1 - \gamma < 0$. Usually, solid particles suspended in a fluid are $\rho > \rho_0$ and $\beta < \beta_0$, so $B + 1 - \gamma > 0$. Then the particles are trapped at the nodes of sound pressure generated every half-wavelength, as shown in Fig. 1.

3. Experiments

3.1. Trapping of particles in a standing wave field

The experimental setup is shown in Fig. 2. A plane-type transducer (resonant frequency 1.75 MHz, diameter 20 mm) is fixed at the bottom of a water tank facing upward and a reflector is placed above it which is parallel to the transducer. The transducer is driven by a continuous sinusoidal wave of 1.75 MHz. When an alumina suspension with average particle diameter of 16 μm was injected into the standing wave field generated between the transducer and the reflector, the particles were trapped in a wide range near the sound beam axis [10]. The density variation of the medium in the sound field was visualized optically using the schlieren technique. Figure 3(a) shows that the sound pressure nodes spread two-dimensionally in the direction perpendicular to the sound beam axis.

To trap the particles at any position in the standing wave field, the sound field must be strong in a narrow region. Since ultrasound converges acoustic energy by means of a concave spherical transducer, a sound field having high sound pressure can be generated near the focal point. If a reflector is placed at the focal point of the concave transducer and a standing wave field is generated, the trapping range of particles can be limited to a narrow region.

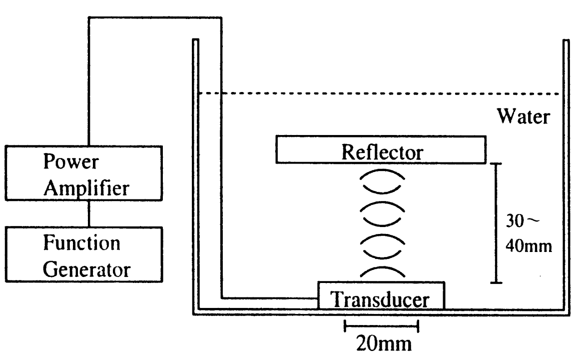

Fig. 2. Experimental apparatus for trapping of particles in an ultrasonic standing wave field.

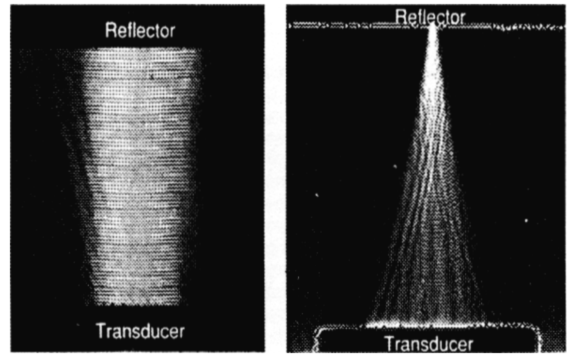

(a) Plane-type transducer (b) Concave spherical transducer

Fig. 3. Schlieren images of the ultrasonic standing wave fields.

Figure 3(b) is a schlieren image of the standing wave field generated in this way. This picture verifies that formation of standing waves is possible even in the case of a concave transducer, and that the sound waves radiated from the transducer are focused and the acoustic energy density increases with distance from the transducer.

When alumina particles were injected into the standing wave field, a large number of particles were trapped in a wide range of the sound field. But, if the sound field was changed by slightly varying the frequency, most of the particles settled due to the gravity force and only particles on the central axis and near the focal point (near the reflector) remained, arranging themselves at half-wavelength intervals.

3.2. One-dimensional transport of agglomerated particles due to frequency change

A transducer has a specific resonant frequency and the efficiency of electroacoustic conversion is lowered if the frequency deviates from resonance. Figure 4 shows the frequency characteristics of the received sound pressure at distances of l = 20, 40 (focal point), and 60 mm on the sound beam axis, where the voltage applied to the transducer was 40 V_{pp}. Taking a peak value at the resonant frequency, the sound pressure decreases with the change in frequency, but this change is relatively slow. For example, a sound pressure above 100 kPa at the focal point can be obtained in a wide frequency range of between 4.5 to 7 MHz. Since an alumina particle 16 μm in diameter has a volume of $V = 2.14 \times 10^{-21}$ m^3 and a mass of 8.41×10^{-12} kg, its weight in water is 83.0 pN and its buoyancy is 21.0 pN, so that a net force of 62.0 pN acts in the downward direction. The sound pressure amplitude A which is required to get a force of more than

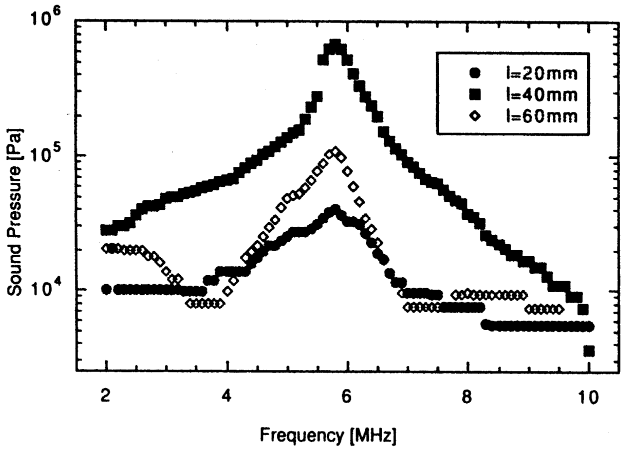

Fig. 4. Frequency characteristics of the concave spherical transducer.

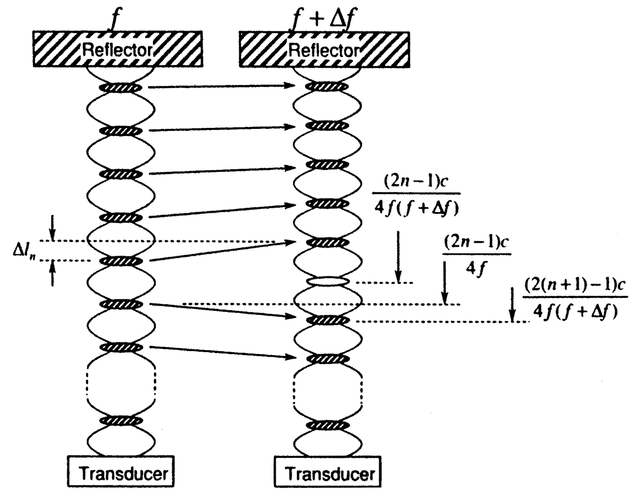

Fig. 5. Behavior of the particles when the frequency changes.

62.0 pN, from the antinode to the node of the sound pressure on the sound beam axis, is more than 41.7 kPa at 4.5 MHz and is 33.4 kPa at 7 MHz. Thus, it would be possible to change the frequency in this range while trapping particles at the focal point. Although the force due to acoustic radiation pressure is lowered with distance from the focal point, the spatial region and the frequency range in which the objects are trapped can be enlarged by increasing the voltage applied to the transducer.

By changing the frequency, the wavelength of the sound is changed and the particles can be moved corresponding to the shift of node of the sound pressure distribution. Figure 5 shows a schematic diagram of the transport of a particle when frequency is changed from f to $f + \Delta f$.

Figure 6 shows the case when the frequency is changed from 4.0 MHz to 8.0 MHz in 0.01-MHz steps in the experiment. Since the amount of the transport is the sum of the variations of the interval between particles, the particles near the reflector do not move much, but the particles away from the reflector move longer distances in proportion to their distances from the reflector. The distance l_n for the n-th particle from the reflector is given by

$$l_n = (2n-1)\lambda/4 = (2n-1)c_0/4f \qquad (8)$$

When the frequency increment Δf is sufficiently small, the transport distance Δl_n of the particle, with frequency change from f to $f + \Delta f$, is given by

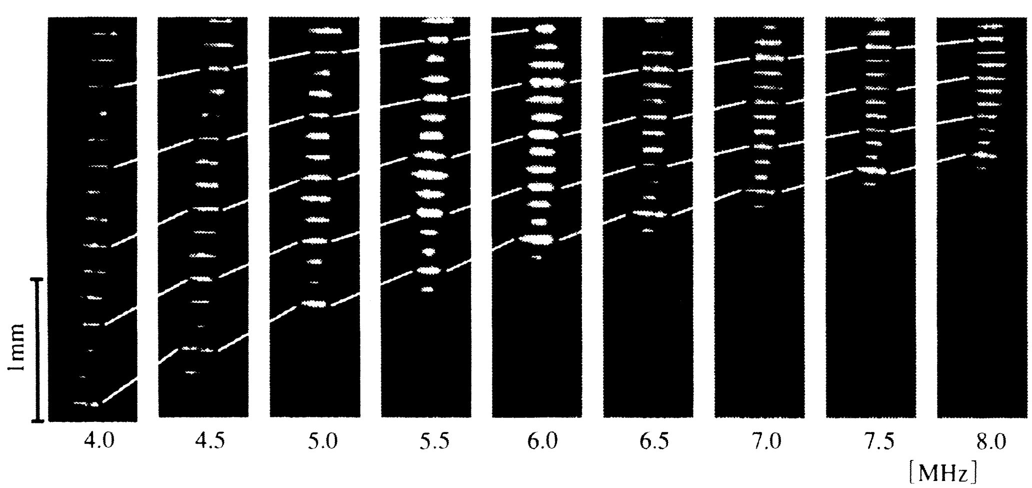

Fig. 6. Transportation of the agglomerated particles due to frequency changes.

$$\Delta l_n = l_n(f) - l_n(f+\Delta f) = (2n-1)c_0 \Delta f / 4f(f+\Delta f) \quad (9)$$

The displacement Δl_n is proportional to n and Δf and is inversely proportional to the square of f.

In the present experiment, the interval between agglomerated particles was from 186 µm to 94 µm depending on the frequency and the change of agglomeration interval associated with a frequency increment of 0.01 MHz was from .46 µm to 0.12 µm. The transport distance of particles is the summation of this change; it increases with distance from the focal point. At the same time, the force acting to trap particles becomes weaker with distance from the focal point and trapping becomes impossible. In the present experiment, the particle trapped at the farthest point from the focal point was transported a distance of about 1.875 mm when the frequency was changed from 4.0 MHz to 8.0 MHz. Here, the resolution of transportation was roughly from 9.4 µm to 2.3 µm when the frequency was changed by an increment of 0.01 MHz. By decreasing the frequency increment, submicrometer resolution may be realized.

3.3. Separation and combination of agglomeration column due to stepwise change of frequency

By changing the frequency in stepwise fashion, an agglomeration column of particles can be separated. As described above, the particles trapped at the sound pressure nodes away from the reflector are transported over a longer distance than the closer particles. However, if the transport distance corresponding to one cycle of the frequency change is greater than half the agglomeration interval (a half-wavelength), the adjacent node on the opposite side becomes closer, and the particle moves in the opposite direction (for example in Fig. 5, particles after the sixth position from the top). To move the n-th particle upward from the reflector when the frequency f is increased, one should have

$$\Delta l_n < \lambda' / 4 \quad (10)$$

or the frequency increment Δf should satisfy the following condition:

$$\Delta f < f / (2n-1) \quad (11)$$

If Δf is greater than this, the n-th particle moves downward. Here λ' is the sound wavelength for the frequency $f + \Delta f$.

Figure 7 shows the behavior of particles when the frequency is changed from 5.0 MHz to 6.0 MHz in steps of 0.10 and 0.20 MHz. When the frequency was increased in steps of 0.05 MHz, all of the particles in the figure moved upward. But when frequency increments of 0.10 and 0.20 MHz were used, the particles at the 25-th and 13-th positions from the reflector, respectively, had transport distances larger than half the agglomeration interval (a half-wavelength). Since the nearer sound pressure node was on the opposite side, the particles moved in the opposite direction. Moreover, when the frequency was decreased, the particles trapped at the adjacent sound pressure nodes accumulated at the same sound pressure nodes.

Thus, by changing the frequency stepwise in a standing wave field using a focused sound source, small objects arranged in a one-dimensional column at the sound pressure node can be separated at an arbitrary boundary or can be accumulated at any point. Using a plane sound source, particles distributed in a wide range can be manipulated. Yamakoshi [16] used a standing wave generated by the intersection of traveling waves from two sound sources. He increased the frequency continuously and the operation of

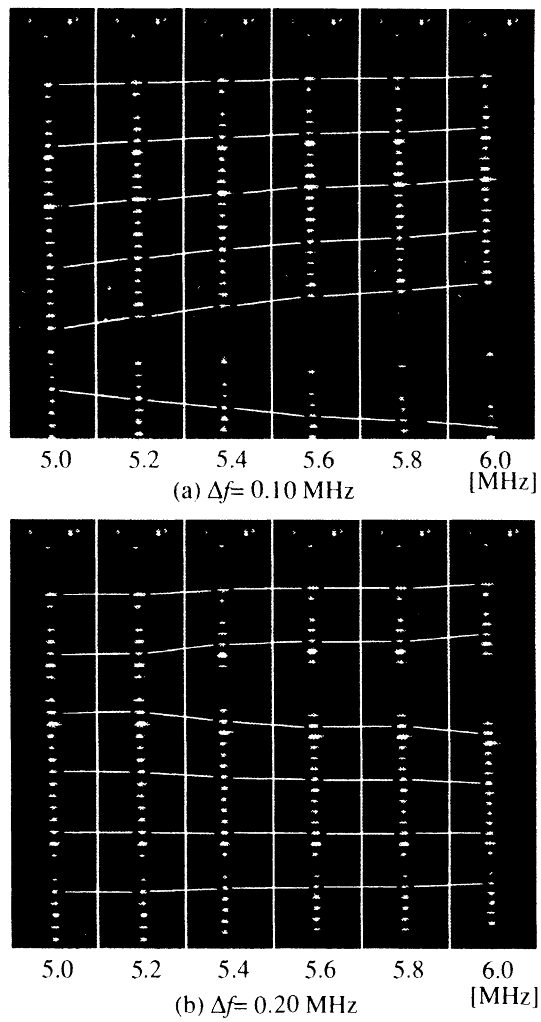

Fig. 7. Separation of the agglomeration column depending on the frequency increment.

returning to the initial value was repeated. In this way the particles in a cell placed in the sound field were accumulated. Benes and colleagues [17] used a series of resonant frequencies so that the distance between the transducer and the reflector was an integral multiple of the half-wavelength. The frequency was increased in steps and the operation of returning to the initial value was repeated. In this way small suspended particles were concentrated with high speed near the transducer and reflector.

4. Discussion

To trap particles at a fixed point, a sharp well of the potential is required in the radial direction and a small variance σ^2 of Gaussian distribution is desirable in Eq. (7). Although σ^2 decreases from the transducer to the reflector at the focal point in the standing wave field of a concave spherical transducer, the region with small σ^2 should be distributed longer along the sound beam axis to increase the transport distance of the trapped objects. Figure 8 shows two-dimensional sound pressure distributions of the traveling wave fields radiated by concave transducers with different curvatures (frequency: 4.5 MHz, diameter: 20 mm, radius of curvature: 30, 40, 50 mm), which were measured with a PVDF hydrophone 1 mm in diameter, on a grid with 1-mm spacing. The abscissa shows the radial distance from the central axis of the transducer and the ordinate shows the longitudinal distance from the transducer. The region of high sound pressure is thin and extended along the central axis of the transducer in each case, but with an increase in the radius of curvature, the region of high sound pressure becomes longer.

In the cross section perpendicular to the axis of the sound beam at the focal point of a concave transducer with aperture radius a_1 and radius of curvature l_f, the sound pressure distribution has the shape of concentric circles. The diameter l_d of the first nodal circle where the sound pressure drops to zero for the first time is given by

$$l_d = 1.2\lambda l_f / a_1 \tag{12}$$

84% of the total acoustic power passes through this circle [18]. The focal zone l_z defined by –6 dB from the sound pressure peak along the sound axis is given by

$$l_z = 4 l_f^2 / (2 l_{near} + l_f) \tag{13}$$

where l_{near} is defined by $l_{near} = a_1 2/\lambda$ and is the region of the near field. Both l_d and l_z increase with the radius of curvature and decrease with the increasing frequency. However, their ratio is

$$\frac{l_d}{l_z} = \frac{0.6 a_1}{l_f} + \frac{0.3\lambda}{a_1} \tag{14}$$

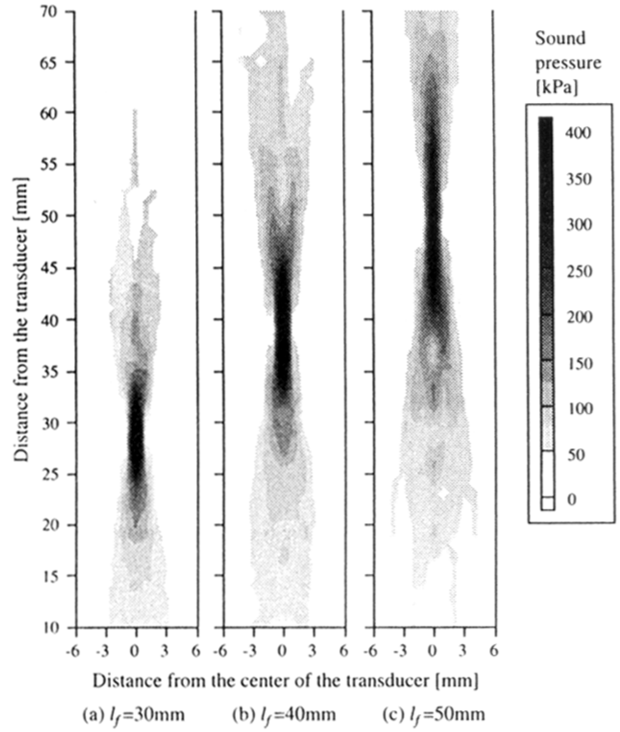

Fig. 8. Variation of sound pressure distribution depending on l_f of the transducer.

and l_d / l_z becomes smaller with an increase in the radius of curvature or an increase in frequency. Thus, a one-dimensional long, thin sound field can be formed.

5. Conclusions

Trapping of small alumina particles suspended in water by means of the acoustic radiation pressure in the standing wave field was investigated. The small particles were agglomerated at the nodes of the sound pressure distribution at half-wavelength intervals and columns were formed along the sound beam axis. When a plane circular transducer was used, the force acting to trap the particles was the strongest near the beam axis, but it was difficult to fix the trapped particles at a particular position since this force acts in a wide range in front of the transducer. By using a concave spherical transducer and placing a plane reflector at the focal point perpendicular to the sound axis, a standing wave field was generated and it became possible to fix the agglomerated particles one-dimensionally. Moreover, by changing the frequency, the trapped particles were transported one-dimensionally along the beam axis and the columns of trapped particles were separated and transported in opposite directions by selecting an appropriate frequency increment. Although the transport distance of the particles varies with the distance from the reflector, the particles can be transported a few millimeters with submicrometer resolution. By controlling the sound field in this way, noncontact micromanipulation is possible with ultrasound.

REFERENCES

1. Esashi M. Micromachines made by silicon technology. Trans J Soc Mech Eng 1996;62:417–422. (in Japanese)
2. Fukuda T, Mitsuoka T. Micro robot of dream. Ohm Press; 1995. (in Japanese)
3. Watanabe T. Electrostatic agglomeration of submicron particles. Proc Inst Electrostatics Jpn 1992;16:483–492. (in Japanese)
4. Ashkin A. Acceleration and trapping of particles by radiation pressure. Phys Rev Lett 1970;24:156–159.
5. Takeuchi M, Abe H, Yamanouchi K. Ultrasonic micromanipulator using visual feedback. Jpn J Appl Phys 1996;35:3244–3247.
6. Yasuda K, Kiyama M, Umemura S. Deoxyribonucleic acid concentration using acoustic radiation force. J Acoust Soc Am 1996;99:1248–1251.
7. Whitworth G, Coakley WT. Particle column formation in a stationary ultrasonic field. J Acoust Soc Am 1992;91:79–85.
8. Whitworth G, Nyborg WL. A rotating ultrasonic waveguide for studying acoustic radiation forces on particles. J Acoust Soc Am 1991;90:2091–2096.
9. Negishi K, Takagi K. Tyoonpa Gijutsu. Tokyo University Press; 1984. p 59–69. (in Japanese)
10. Kozuka T, Tuziuti T, Mitome H, Fukuda T. Noncontact micro manipulation using an ultrasonic standing wave field in water. Trans J Soc Mech Eng (C) 1997;63:1279–1286. (in Japanese)
11. Wu J. Acoustical tweezers. J Acoust Soc Am 1991;89:2140–2143.
12. Wu J, Du G. Acoustic radiation force on a small compressible sphere in a focused beam. J Acoust Soc Am 1990;87:997–1003.
13. Nyborg WL. Radiation pressure on a small rigid sphere. J Acoust Soc Am 1967;42:947–952.
14. Gor'kov LP. On the forces acting on a small particle in an acoustical field in an ideal fluid. Soc Phys Dokl 1962;6:773–775.
15. Takeuchi M. Ultrasonic micromanipulation of micro-sized particles. J IEICE 1996;79:1213–1218. (in Japanese)
16. Yamakoshi Y. Measurement technique utilized radiation pressure for micro particles. J Acoust Soc Jpn 1996;52:210–216. (in Japanese)
17. Benes E, Hager F, Bolek W, Gröschl. Separation of dispersed particles by drifting ultrasonic resonance fields. Ultrasonics Int 91 Conf Proc. Oxford: Butterworth–Heinemann; p 167–170.
18. Saneyoshi J, Kikuchi Y, Nomoto O. Tyoonpa Gijutsu Binran (Ultrasonic handbook). Nikkei Kogyo Newspaper Co; 1978. p 166–174. (in Japanese)

AUTHORS (from left to right)

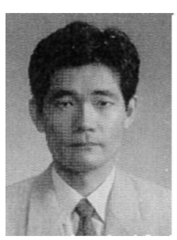

Teruyuki Kozuka (member) received his B.E. degree in electrical engineering from Aichi Institute of Technology in 1986. He then joined the National Industrial Research Institute of Nagoya where he is a senior researcher. He has been doing research on applications of acoustic radiation pressure using underwater ultrasound. He is a member of the Institute of Electrical Engineers of Japan, the Japan Society of Mechanical Engineers, and the Acoustical Society of Japan.

Toru Tuziuti received his M.S. degree in physics from the Science University of Tokyo in 1993. He then joined the National Industrial Research Institute of Nagoya. He has been doing research on optical visualization of ultrasonic fields and its analysis. He is a member of the Acoustical Society of Japan and the Society of Powder Technology, Japan.

AUTHORS (continued) (from left to right)

Hideto Mitome received his Ph.D. degree in aeronautical engineering from Nagoya University in 1979. He then joined the Mechanical Engineering Laboratory, AIST. In 1991, he moved to the National Industrial Research Institute of Nagoya. His research area is mainly nonlinear acoustics. He is a member of the Acoustical Society of Japan, the Acoustical Society of America, the Marine Acoustics Society of Japan, and the Japan Society of Mechanical Engineers.

Toshio Fukuda received his B.E. degree in mechanical engineering from Waseda University in 1971. He obtained his Ph.D. degree from the University of Tokyo and then joined the Mechanical Engineering Laboratory. He became a lecturer at the Science University of Tokyo in 1982 and became an assistant professor in 1983. He served as a visiting associate professor at Yale University in 1986. He became a professor at Nagoya University in 1989. He has been doing research on robots for special environments.